NANO LETTERS

Letter

pubs.acs.org/NanoLett

Efficient Light Trapping in Inverted Nanopyramid Thin Crystalline Silicon Membranes for Solar Cell Applications

Anastassios Mavrokefalos, Sang Eon Han, Selcuk Yerci, Matthew S. Branham, and Gang Chen*

Department of Mechanical Engineering, Massachusetts Institute of Technology, 77 Massachusetts Avenue, Cambridge Massachusetts 02139, United States

ABSTRACT: Thin-film crystalline silicon (c-Si) solar cells with light-trapping structures can enhance light absorption within the semiconductor absorber layer and reduce material usage. Here we demonstrate that an inverted nanopyramid light-trapping scheme for c-Si thin films, fabricated at wafer scale via a low-cost wet etching process, significantly enhances absorption within the c-Si layer. A broadband enhancement in absorptance that approaches the Yablonovitch limit (Yablonovitch, E. *J. Opt. Soc. Am.* **1987**, *72*, 899−907) is achieved with minimal angle dependence. We also show that c-Si films less than 10 μm in thickness can achieve absorptance values comparable to that of planar c-Si wafers thicker than 300 μm, amounting to an over 30-fold reduction in material usage. Furthermore the surface area increases by a factor of only 1.7, which limits surface recombination losses in comparison with other nanostructured light-trapping schemes. These structures will not only significantly curtail both the material and processing cost of solar cells but also allow the high efficiency required to enable viable c-Si thin-film solar cells in the future.

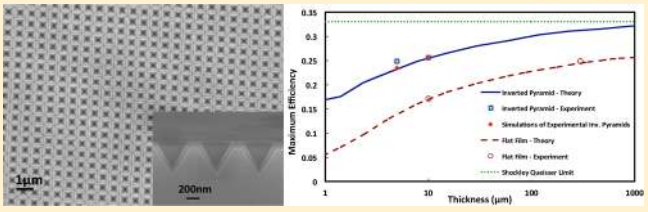

KEYWORDS: *Light trapping, photovoltaics, optical absorption, inverted pyramids, thin-film solar cells*

Bulk crystalline silicon (c-Si) solar cells dominate the photovoltaic (PV) market. Typically, c-Si wafers 180−300 μm thick are used to ensure adequate absorption of sunlight, and this material accounts for about half of the total module cost.[2,3] In bulk crystalline Si solar cells, light trapping is typically provided by randomly textured surfaces.[4] The characteristic size of these textures is typically 3−10 μm, which is much larger than the wavelength of sunlight and not applicable for thin films. Thus various nanophotonic structures have been studied in recent years, including nanowires, nanoholes, nanocones, plasmonic particles, and photonic crystal surface structures.[5−14] The efficiency of Si nanowire- and nanohole-based solar cells[6,7,15−17] has been limited to ∼10%, a value far smaller than the ∼25% efficiency for state-of-the-art thick c-Si solar cells.[18] One major reason for the low efficiency in solar cells with nanowires and nanoholes is the high surface recombination rates due to the large surface area, which is usually more than an order of magnitude larger than flat cells.[19] It was recently reported that flat 10−20 μm thick c-Si based solar cells can have conversion efficiencies up to 15%.[20,21] Our previous work investigating nanopyramid structures through simulation has shown great promise to enhance light absorption in thin c-Si based solar cells while minimizing the surface area increase. In this letter, we experimentally show that c-Si thin films with thicknesses less than 10 μm can absorb as well as 300 μm thick flat c-Si substrates when they are decorated with inverted nanopyramid structures.

We recently investigated various light-trapping structures based on crystalline Si materials, such as nanowires, nanoholes, pyramids, and inverted pyramids through numerical simulation.[22−24] Of all these structures, inverted nanopyramids possess three major advantages for experimental demonstration: (1) They enable films that are less than 10 μm thick to achieve similar efficiencies to bulk c-Si cells with a thickness >300 μm; (2) The surface area increase is only 1.7 times compared to flat surfaces, which minimizes surface recombination losses; and (3) The fabrication of the structures is easy and cost-effective.

We fabricated inverted nanopyramids using standard scalable microfabrication techniques based on interference lithography (IL)[25] and wet Si etching.[26] Figure 1a shows an optical image of the typical sample. The exposed area is limited by the exposure area of the IL tool to approximately 25 ×25 mm. It should be noted that IL can be applied to standard 156 × 156 mm wafers.[27] Typical scanning electron microscope (SEM) images of the resulting structures are illustrated in Figure 1b,c. Figure 1b illustrates the top view of inverted nanopyramids with a periodicity of 700 nm and a mean separation of 100 nm between the pyramids produced after etching in a potassium hydroxide (KOH) solution. Figure 1c illustrates the cross-sectional SEM of the resulting structure with the insets clearly showing the interfaces of the SiN_x, Si, SiO_2, and Ag layers. The sample illustrated here employed a 90 nm-thick SiN_x, 10 μm-thick Si, 1 μm-thick SiO_2, and 200 nm-thick Ag as antireflection coating, active absorbing medium, surface passivation, and back reflector, respectively. Because of the anisotropic etching of c-Si in the KOH solution, inverted nanopyramids are formed at an

Received: December 29, 2011
Revised: May 18, 2012
Published: May 21, 2012

   dx.doi.org/10.1021/nl2045777 | *Nano Lett.* 2012, 12, 2792−2796

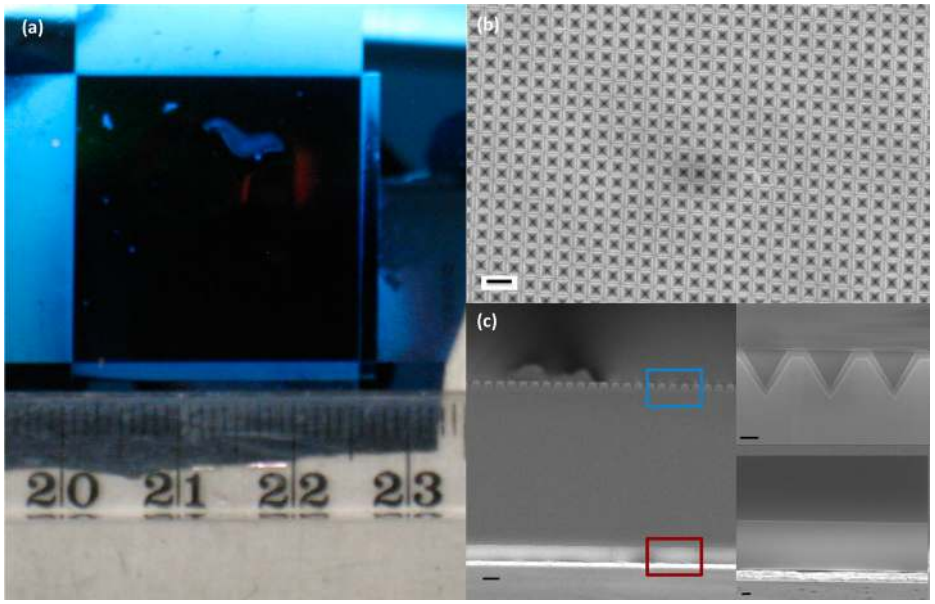

Figure 1. (a) Optical, (b) top view SEM, and (c) cross-sectional SEM images of the 10 μm c-Si film illustrating the patterned inverted nanopyramids on a 700 nm period. A 90 nm SiN_x layer is deposited on the inverted pyramids, and a SiO_2 (1 μm) and a silver (200 nm) layer are at the backside of the c-Si film. The right bottom insets are close-ups of the blue and red boxed regions. The scale bars in both (b) and (c) are 1 μm. The scale bars in the insets in (c) are 200 nm.

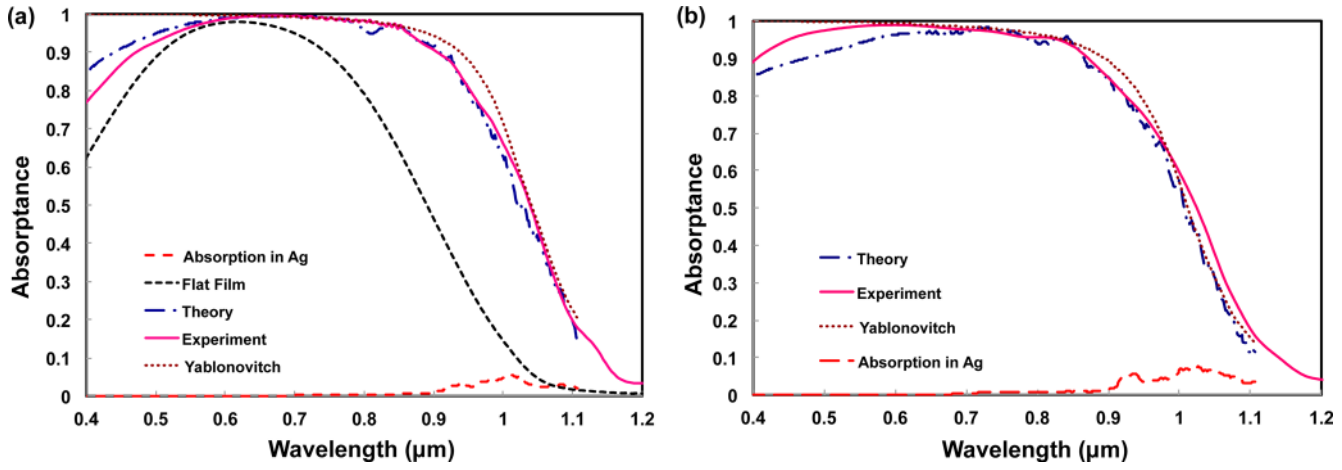

Figure 2. Comparison of the theoretical and experimental absorptance spectra, the Yablonovitch limit corresponding to the c-Si thickness, and the calculated absorptance in the Ag layer for film thicknesses of (a) 10 μm (the structure of Figure 1) and (b) 5 μm, respectively. The experimental absorptance spectrum for a flat film is included in (a) as a baseline. The dimensions of the flat film structure are 70 nm SiN_x, 10 μm Si, 250 nm SiO_2, and 200 nm Ag in thickness. In (b), the inverted pyramid structure consists of 90 nm SiN_x, 5 μm Si, 0.5 μm SiO_2, and 200 nm Ag. The Yablonovitch limit was obtained by considering a c-Si film on the SiO_2 and Ag layers of the same thickness, as in the corresponding inverted pyramid structures. Note that, except for the Ag absorption curves, the other absorptance spectra account for absorption in all layers. For all the theoretical curves, the spectra were averaged over a wavelength range to smoothen sharp peaks.

angle of 54.7° to the wafer surface, which is responsible for the factor of 1.7 increase in surface area.

We carried out absorption measurements for the structure shown in Figure 1 using a spectrophotometer attached to an integrating sphere. Figure 2a shows the experimental results measured at 8° from the surface normal compared to the simulated results at 10°. Simulations were carried out using the transfer matrix method.[28] The experimental results show good agreement with the theoretical predictions over almost the entire spectrum. The deviations at short wavelengths are most likely due to the variation in the separation distance between pyramids (ridge size). Samples of varying ridge size yielded absorptance fluctuations that are most pronounced at short wavelengths. Close up SEM images showed that the separation between successive pyramids is approximately 100 nm with fluctuations of ~10 nm for the sample shown in Figure 1. Furthermore, the thickness variations of the SiN_x layer deposited on inverted nanopyramids limit simulation of the exact structure. As a baseline, we also measured the absorptance of a flat 10 μm Si film coated with a 70 nm SiN_x antireflection coating. The film with inverted nanopyramids shows a clear absorption enhancement throughout the solar spectrum compared to the flat film, demonstrating the light-trapping benefit of inverted nanopyramids. Moreover, based on the calculations, we found that absorption in the silver layer is negligible compared to absorption in Si as shown in Figure 2.

dx.doi.org/10.1021/nl2045777 | *Nano Lett.* 2012, 12, 2792–2796

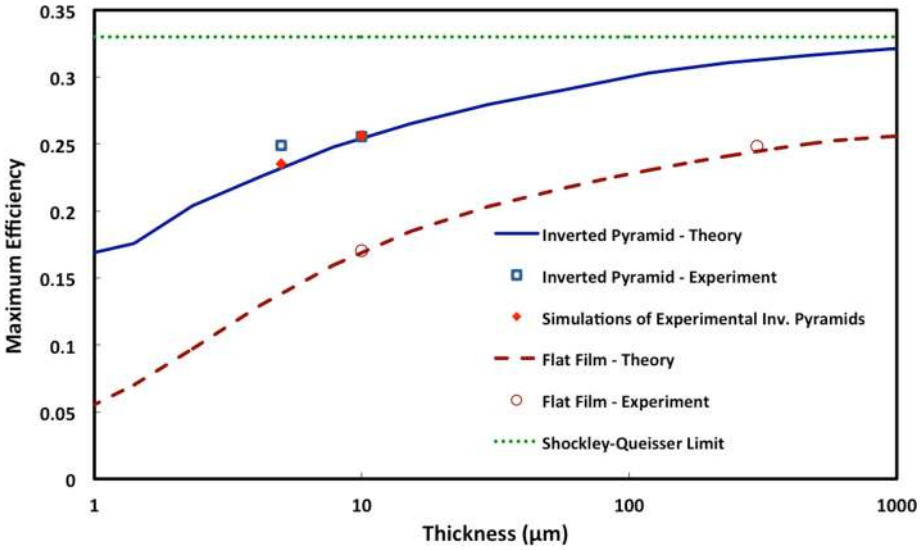

Figure 3. Maximum efficiency at normal incidence as a function of thickness for simulated inverted nanopyramids (blue solid line) and a planar film (brown dashed line) with 90 and 63 nm SiN_x antireflection coatings, respectively. The blue open squares represent the experiments for inverted nanopyramids and the brown open circles the experiments for flat films at 8° incidence angle. The red diamonds represent the simulated maximum efficiency for the structures used in experiments at the incidence angle of 10°. The dotted green line is the maximum theoretical Shockley–Queisser efficiency. The experimental results were obtained by subtracting the calculated absorptance in Ag from the measured total absorptance, a small correction of less than 1% in maximum efficiency.

The absorptance of the thin film c-Si layer with inverted nanopyramids is close to the Yablonovitch limit,[1] confirming the effectiveness with which they trap photons. Absorption in periodic surface structures can indeed exceed the Yablonovitch limit for a particular angle of incidence but not in the case of isotropically incident radiation.[13] The calculations are performed for wavelengths up to 1.1 μm, which corresponds to the band gap of c-Si.

We also fabricated inverted nanopyramids using a 5 μm-thick c-Si film with an average ridge size of 50 nm and measured the absorption spectrum as shown in Figure 2b. The experimental absorptance matches well with theoretical predictions; the variations at short wavelengths can be attributed to the same effects as described earlier for 10 μm-thick films.

To fully gauge optical absorption enhancement, we calculated the maximum photovoltaic efficiency, following the treatment developed by Shockely and Queisser,[29] of our structures based on the calculated and measured absorptance in the Si films. This is the efficiency of a photovoltaic cell at room temperature when only radiative recombination of charge carriers occurs among other mechanisms. We assumed that the radiation intensity due to carrier recombination is Lambertian and constructed its angular dependence based on the radiation intensity in the surface normal. In the calculations, AM1.5G solar flux[30] was used for incident light. Experimental and theoretical maximum efficiency values are plotted in Figure 3 for: (1) 5 and 10 μm films with inverted nanopyramids presented earlier (experiment); (2) 10 and 300 μm flat films (experiment); and (3) 5 and 10 μm-thick films consisting of inverted nanopyramids with a ridge separation of 50 and 100 nm, respectively (theory). Additionally, theoretical maximum efficiency curves are plotted as a function of thickness for a flat film and a film with inverted nanopyramids with no ridge spacing. Also plotted in the figure is the Schockley–Queisser limit assuming all incident photons above the bandgap are absorbed. For the experimental results, we obtained the absorptance of the silicon layer by subtracting the calculated absorptance in Ag from the total measured absorptance. The calculated absorptance in Ag is based on the measured dielectric function of the deposited Ag layer obtained using ellipsometry. There is excellent agreement between the experimental data and the theoretical curves for both inverted nanopyramids and flat films, as shown in Figure 3. The small difference between theory and experiment for the absorptance of inverted nanopyramids can be related to the ~10 nm variation in ridge separation as noted earlier. The effect of a 10 nm variation in ridge size is more pronounced for the film with a 50 nm ridge gap than for the one with a 100 nm ridge gap because of the proportionally greater variation in the ridge width. Based on the maximum efficiency measurements and calculations, the 5 and 10 μm-thick films with inverted nanopyramids can absorb light with efficiencies similar to those of planar films that are 300 μm thick. Therefore, inverted nanopyramids can yield an order of magnitude reduction of silicon mass.

Figure 4 illustrates the measured and simulated angular dependence of maximum efficiency for the structure demonstrated in Figure 1. We can clearly see that the theoretical maximum efficiency is almost independent of the angle of incidence up to 40° and is validated by our experiments. The inset shows the angular dependence of absorptance for the structure shown in Figure 1 taken with a variable angle attachment in the integrating sphere (see method).

Finally, Figure 5 shows what the expected short circuit current would be for each one of our experimental structures, based on 100% internal quantum efficiency (i.e., every photon that is absorbed will contribute to the current of the cell in short-circuit mode). The short-circuit current of 37.5 mA/cm^2 for the 10 μm and 37.1 mA/cm^2 for the 5 μm thick samples with inverted nanopyramid structures is close to their respective Yablonovitch limit values of 39.4 mA/cm^2 (10 μm thick) and 37.4 mA/cm^2 (5 μm thick). Furthermore they are significantly higher than the short current of 29.5 mA/cm^2 for a 10 μm-thick flat film with optimized antireflection coating and comparable

dx.doi.org/10.1021/nl2045777 | Nano Lett. 2012, 12, 2792–2796

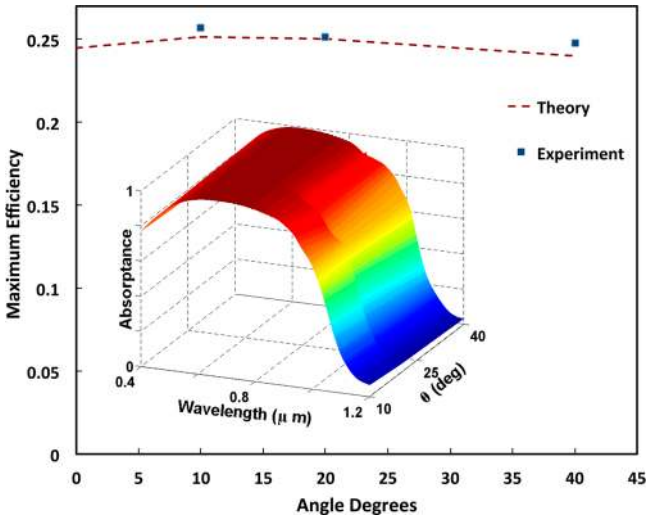

Figure 4. Comparison of experimental and simulated maximum efficiency for the structure shown in Figure 1 at different incidence angles. Inset is the experimental light absorptance for the structure of Figure 1 measured at incidence angles of 10°, 20°, and 40°.

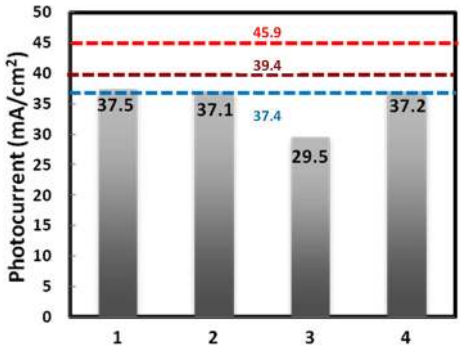

Figure 5. Comparison of the short circuit currents generated by our four structures (gray bars), the Yablonovitch limits for 5 and 10 μm (blue and brown dashed lines, respectively) thick silicon films, and full absorption in silicon (red dashed line).

to the value of 37.2 mA/cm^2 for the 300 μm-thick flat film with optimized antireflection coating.

In conclusion we experimentally and theoretically investigated the light-trapping properties of periodic inverted nanopyramid structures on thin c-Si films fabricated by a microfabrication process based on interference lithography. Through optical characterization, we demonstrated that inverted nanopyramids significantly enhance light absorption above the silicon bandgap across the solar spectrum in thin c-Si films with respect to planar films. This enhancement is almost independent of angle of incidence and approaches the Yablonovitch limit. Our work suggests that one can achieve solar cell efficiencies in c-Si thin films comparable to their bulk counterparts, enabling a reduction of silicon material usage by 1 order of magnitude.

Methods. *Inverted Nanopyramid Fabrication.* The fabrication process flow is as follows: First, a commercial silicon-on-insulator (SOI) wafer was acquired with the desired Si and SiO_2 thicknesses. Then an array of holes was patterned in negative photoresist on the surface of the Si thin film using IL. Subsequent wet etching in an aqueous KOH solution was used to produce the inverted pyramids on the surface of the Si thin film and etch the backside of the Si handle wafer. KOH wet chemistry was chosen because it etches c-Si anisotropically yielding a self-aligned pyramid structure. Finally a SiN_x antireflection coating was deposited on top of the inverted pyramids with plasma enhanced vapor deposition (PECVD), and a silver layer was deposited by evaporation on the backside of the SiO_2 to simulate the Ag back contact of the photovoltaic module.

Optical Measurements. Integrated reflection measurements were carried out with a Perkin-Elmer LAMBDA 950 UV−vis/NIR spectrophotometer system using a 150 mm integrating sphere attachment. The spectrophotometer uses a holographic grating monochromator with 1440 lines/mm UV−vis blazed at 240 nm, 360 lines/mm NIR blazed at 1100 nm, a wavelength range from 175−3300 nm, and a 3−120 mm spot height. The integrating sphere measures the total reflection (R) of the light incident on a surface, including both specular and diffuse components. Because the samples measured here have a Ag metal layer on the back to prevent light transmission, the absorptance (A) of the final structure can be simply calculated from the $A = 1 - R$, where R is the reflectance. The measurement covered the solar spectrum that is useful for c-Si with a bandgap of 1.1 eV. The measurements of the angle dependence of absorptance were carried out using the variable angle center-mount option in which the sample is suspended in the middle of the sphere. Spectroscopic ellipsometry measurements were performed to obtain the thickness and optical constants of silicon nitride layers deposited on flat silicon films. The Δ and Ψ values were measured using a J. A. Woollam Co. variable-angle spectroscopic ellipsometer (VASE) in a spectral range 400−1200 nm. The silicon nitride data were analyzed using the Cauchy−Urbach model.[31] Silver films deposited on SOI wafers were also analyzed by spectroscopic ellipsometry using the default model for Ag in the VASE library which yielded similar values for the refractive index and absorption coefficient of Ag compared to values in the literature.[32]

AUTHOR INFORMATION

Corresponding Author

*E-mail: gchen2@mit.edu

Notes

The authors declare the following competing financial interest(s): A patent has been filed based on this work.

ACKNOWLEDGMENTS

We thank T. Buonassisi and J. Sullivan at MIT for helping with the optical measurements. This research was supported by DOE Sunshot Project under DOE Award No. DEEE0005320 (A.M, S.Y., S.E.H.), Nanoscale Science and Engineering Initiative of the National Science Foundation under NSF award no. CMMI-0751621 through the Center for Scalable and Integrated Nano-247 manufacturing at U. C. Berkeley (M.B.). A.M. was supported by the Postdoctoral fellowship in the Cyprus Institute Program for Energy Environment and Water Resources (CEEW) at the MIT Laboratory for Energy and the Environment (LFEE).

REFERENCES

(1) Yablonovitch, E. *J. Opt. Soc. Am.* **1987**, *72*, 899−907.
(2) Green, M. A. *J. Mater. Sci.: Mater. Electron.* **2007**, *18*, S15−S19.
(3) Brendel, R. *Sol. Energy* **2004**, *77*, 969−982.
(4) Campbell, P.; Green, M. A. *J. App. Phys.* **1987**, *62*, 243−249.
(5) Kelzenberg, M. D.; et al. *Nat. Mater.* **2010**, *9*, 239−44.
(6) Peng, K. Q.; et al. *Small* **2005**, *1*, 1062−1067.

(7) Peng, K. Q.; Wang, X.; Li, L.; Wu, X. L.; Lee, S. T. *J. Am. Chem. Soc.* **2010**, *132*, 6872−3.
(8) Atwater, H. A.; Polman, A. *Nat. Mater.* **2010**, *9*, 205−13.
(9) Munday, J. N.; Atwater, H. A. *Nano Lett.* **2011**, *11*, 2195−201.
(10) Pillai, S.; Catchpole, K. R.; Trupke, T.; Green, M. A. *J. Appl. Phys.* **2007**, *101*, 8.
(11) Stuart, H. R.; Hall, D. G. *Appl. Phys. Lett.* **1996**, *69*, 2327−2329.
(12) Hsu, C. M.; Connor, S. T.; Tang, M. X.; Cui, Y. *Appl. Phys. Lett.* **2008**, *93*, 133109.
(13) Yu, Z. F.; Raman, A.; Fan, S. H. *Proc. Nat. Acad. Sci. U.S.A.* **2010**, *107*, 17491−17496.
(14) Cao, L.; et al. *Nano Lett.* **2011**, *10*, 439−445.
(15) Tsakalakos, L.; et al. *Appl. Phys. Lett.* **2007**, *91*, 233117.
(16) Muskens, O. L.; Rivas, J. G.; Algra, R. E.; Bakkers, E. P. A. M.; Lagendijk, A. *Nano Lett.* **2008**, *8*, 2638−2642.
(17) Garnett, E.; Yang, P. *Nano Lett.* **2010**, *10*, 1082−1087.
(18) Green, M. A. *Prog. Photovolt.* **2009**, *17*, 183−189.
(19) Kelzenberg, M. D.; et al. *Energy Environ. Sci.* **2011**, *4*, 866−871.
(20) Cruz-Campa, J. L.; et al. *Sol. Energy Mater. Sol.* **2011**, *95*, 551−558.
(21) Yoon, J.; et al. *Nat. Commun.* **2011**, *2*, 343.
(22) Hu, L.; Chen, G. *Nano Lett.* **2007**, *7*, 3249−52.
(23) Han, S. E.; Chen, G. *Nano Lett.* **2010**, *10*, 1012−5.
(24) Han, S. E.; Chen, G. *Nano Lett.* **2010**, *10*, 4692−6.
(25) Savas, T. A.; Schattenburg, M. L.; Carter, J. M.; Smith, H. I. *J. Vac. Sci. Technol., B* **1996**, *14*, 4167−4170.
(26) Kovacs, G. T. A.; Maluf, N. I.; Petersen, K. E. *Proc. IEEE* **1998**, *86*, 1536−1551.
(27) Mao, W.; Wathuthanthri, I.; Choi, C. H. *Opt. Lett.* **2011**, *36*, 3176−3178.
(28) Pendry, J. B.; Mackinnon, A. *Phys. Rev. Lett.* **1992**, *69*, 2772−2775.
(29) Shockley, W.; Queisser, H. J. *J. Appl. Phys.* **1961**, *32*, 510−519.
(30) *Air Mass 1.5 Spectra*; American Society for Testing and Materials: West Conshohocken, PA; http://rredc.nrel.gov/solar/spectra/am1.5/.
(31) Tompkins, H. G.; Gregory, R. B.; Deal, P. W.; Smith, S. M. *J. Vac. Sci. Technol., A* **1999**, *17*, 391−397.
(32) *Handbook of Optical Constants of Solids*; Palik, E. D., Ed.; Academic: Orlando, FL, 1985.